arXiv:1301.6460v1 [cond-mat.mes-hall] 28 Jan 2013

Making Quantum Spin-Hall Effect Robust via Magnetic Manipulation

Huichao Li[1], L. Sheng[1],[*] L. B. Shao[1], Baigeng Wang[1], D. N. Sheng[2], and D. Y. Xing[1][†]
[1] *National Laboratory of Solid State Microstructures and Department of Physics, Nanjing University, Nanjing 210093, China*
[2] *Department of Physics and Astronomy, California State University, Northridge, California 91330, USA*

(Dated: January 29, 2013)

The quantum spin Hall (QSH) effect is known to be unstable to perturbations violating time-reversal symmetry. We show that creating a narrow ferromagnetic (FM) region near the edge of a QSH sample can push one of the counterpropagating edge states to the inner boundary of the FM region, and leave the other at the outer boundary, without changing their spin polarizations and propagation directions. Since the two edge states are spatially separated into different "lanes", the QSH effect becomes robust against symmetry-breaking perturbations.

PACS numbers: 72.25.-b, 73.43.-f, 73.20.At, 73.50.-h

The quantum spin Hall (QSH) effect, a quantum state of matter, has attracted much attention in recent years, because of its fundamental interest and potential applications in spintronic devices. The QSH effect was first predicted theoretically by Kane and Mele [1] and by Bernevig and Zhang [2], in independent works, and soon after observed experimentally in HgTe quantum wells. [3, 4] A key ingredient to the QSH effect is a strong intrinsic spin-orbit coupling, which acts as spin-dependent magnetic fluxes coupled to the electron momentum. In the ideal case, where electron spin is conserved, the two spin sectors of a QSH system behave like two independent quantum Hall (QH) systems without Landau levels. [5] They contribute opposite quantized Hall conductivities, when the electron Fermi level is inside the bulk band gap, so that the total Hall conductivity vanishes but the spin Hall conductivity is quantized. On a sample edge, two counterpropagating gapless edge modes with opposite spin polarizations exist in the bulk band gap, which can transport spin currents without dissipation of energy.

When the spin conservation is destroyed, e.g., by the Rashba-like spin-orbit coupling, the spin Hall conductivity deviates from the quantized value. [6] However, the edge transport can remain to be dissipationless, [1, 7] provided that the time-reversal (TR) symmetry is present and the bulk band gap is not closed. In this case, a QSH system can no longer be divided into two QH systems, and the existence of the gapless edge states has been attributed to the nontrivial topological properties of bulk energy bands. The nontrivial bulk band topology of the QSH systems is usually described by the Z_2 index [8] or the spin Chern numbers. [9–11] These topological invariants reveal the fundamental distinction between a QSH insulator and an ordinary band insulator.

Extension of the idea of the QSH effect to higher dimension has led to the proposals of three-dimensional (3D) TIs. [12–16] Research of the 3D TIs has been fruitful in recent years, both theoretically and experimentally. A 3D TI has a bulk band gap and gapless surface states on the sample boundary. A simple 3D TI consists of layers of 2D QSH systems. However, such a 3D TI is not stable in the presence of disorder due to interlayer scattering, and so called the weak TI. A strong TI is topologically nontrivial in any direction, and the surface states are characterized by an odd number of Dirac cones. The metallic surface states of the 3D TIs provide a unique platform for realizing some exotic physical phenomena, such as Majorana fermions [17] and topological magnetoelectric effect. [18, 19] The existence of topological surface states in the 3D TIs has been experimentally confirmed in $Bi_{1-x}Sb_x$, Bi_2Te_3, and Bi_2Se_3 materials, [20–25] which evokes a great surge of research interest in this field.

While the TR symmetry was often considered to be a prerequisite to the QSH effect, its role is two-sided. In a TR invariant QSH system, the two oppositely moving edge states at the Fermi energy are connected to each other under TR, and so have opposite spin orientations. Elastic backscattering from nonmagnetic random potential is forbidden. On the other hand, the two opposite movers have identical spatial probability distributions. Turning on small TR-symmetry-breaking perturbations immediately couples the two edge states, giving rise to backscattering. This makes the QSH effect fragile in realistic environments, where perturbations violating the TR symmetry are usually unavoidable. Experimentally, two-terminal conductance close to the predicted value $2e^2/h$ was observed only for small QSH samples with dimensions of about $(1 \times 1)\mu m^2$ [4], in contrast to the traditional QH effect, where the Hall conductivity can be precisely quantized on macroscopic scales. So far, QSH effect as robust as the QH effect has been elusive. It was found recently that the nontrivial bulk band topology of the QSH systems remains intact, even when the TR symmetry is broken, [26] implying that the instability of the QSH effect is solely due to properties of the edge states.

In this Letter, we show that the QSH effect can be stablized by designed removal of the TR symmetry of the edge states. Creating a narrow ferromagnetic (FM) region near one edge of a QSH sample can push one of the counterpropagating edge states to the inner boundary of the FM region, and leave the other on the outer boundary. The moving directions and spin orientations of the individual edge states are unchanged, so that the QSH effect persists. Importantly, the edge states are spatially separated, so that the QSH effect becomes robust against general perturbations without fictitious symmetry constraints. Our work paves a road to realize robust QSH effect via magnetic manipulation.

We start from the effective Hamiltonian for a HgTe quantum well [3] with a uniform FM exchange field, given by

$$H = v_{\rm F}(\hat{\tau}_z k_x \hat{\sigma}_x + k_y \hat{\sigma}_y) + (M_0 - Bk^2)\hat{\sigma}_z + H_1 \ , \qquad (1)$$

where $\hat{\boldsymbol{\tau}}$ stand for Pauli matrices for two spin states, and $\hat{\boldsymbol{\sigma}}$ for the electron and hole bands. An exchange field can be created in the HgTe layer by doping of magnetic atoms, such as Mn, [27] or through magnetic proximity effect with a FM insulator. The exchange field can be described by [27] $H_1 = g_0\hat{\tau}_z\hat{\sigma}_z + g_1\hat{\tau}_z$, where $g_0 = \frac{1}{2}(G_{\rm H} - G_{\rm E})$ and $g_1 = \frac{1}{2}(G_{\rm H} + G_{\rm E})$ with $2G_{\rm E}$ ($2G_{\rm H}$) as the exchange splitting of the electron (hole) bands. For convenience, we set the reduced Planck constant $\hbar$ to be unity, and take the momentum to be dimensionless by properly choosing the units for parameters of the model, namely, $v_{\rm F}$, M_0, B, g_0, and g_1.

It is worth mentioning that the model Hamiltonian Eq. (1) can describe not only the HgTe quantum wells, but also a class of QSH systems. [28] For example, setting $g_1 = 0$ and making a unitary transformation $\mathcal{H} = U^\dagger H U$ with $U = \frac{1}{2}[(1 + \hat{\tau}_z) + (1 - \hat{\tau}_z)\hat{\sigma}_y]e^{-i\frac{\pi}{4}\hat{\sigma}_z}$, we obtain $\mathcal{H} = v_{\rm F}(k_y\hat{\sigma}_x - k_x\hat{\sigma}_y) + \left(M_0 - Bk^2\right)\hat{\tau}_z\hat{\sigma}_z + g_0\hat{\sigma}_z$. One can find that this Hamiltonian is identical to that of a thin film of 3D TI $\mathrm{Bi_2Se_3}$ with an exchange field, [11, 29] for which $\hat{\boldsymbol{\sigma}}$ stand for spin up and down, and $\hat{\boldsymbol{\tau}}$ for bonding and antibonding of the surface states on two surfaces.

Since $\hat{\tau}_z$ is a conserved quantity, one can easily diagonalize Eq. (1), and obtain two conduction bands and two valence bands. Under the condition of $|g_0| > |g_1|$, a nonzero middle band gap exists except at $g_0 = \pm M_0$, where the conduction and valence bands touch. As has been discussed in Ref. [27], for HgTe quantum wells doped with Mn, $G_{\rm E}$ and $G_{\rm H}$ have opposite signs, so that the condition above is always satisfied. The spin Chern numbers for $\tau_z = \pm 1$ can be derived to be

$$C_\pm = \pm\frac{1}{2}[\mathrm{sgn}(B) + \mathrm{sgn}(M_0 \pm g_0)] \ . \qquad (2)$$

At $g_0 = 0$, $C_\pm = \pm\mathrm{sgn}(B)$ if $BM_0 > 0$, corresponding to a QSH phase, and $C_\pm = 0$ otherwise, corresponding to an ordinary insulator. We focus on systems with $BM_0 > 0$, which are in the QSH phase at $g_0 = 0$, and for the sake of definiteness, we will confine ourselves to the parameter region of $B > 0$ and $M_0 > 0$, in which $C_\pm = (1, -1)$ at $g_0 = 0$. (All the conclusions reached in this work do also apply to the case of $B < 0$ and $M_0 < 0$.) Notably, with increasing g_0 to $g_0 = M_0$, $C_\pm$ undergo a transition from $(1, -1)$ to $(1, 0)$.

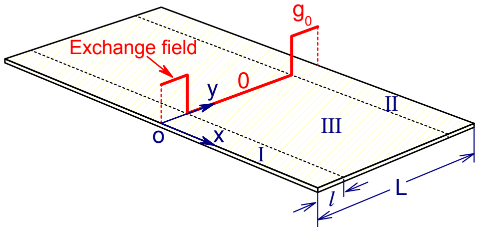

FIG. 1: Schematic of the QSH sample with a long strip geometry. The profile of the y-dependent exchange field is shown by the thick (red) line.

Next we consider a QSH sample with a long strip geometry, as shown in Fig. 1. We will set $g_1 = 0$ for now, which does not affect topological properties of the system in the case of $|g_0| < |g_1|$. The effect of finite g_1 will be discussed later. The exchange field g_0 is taken to be nonzero in narrow regions of width l near the two edges of the strip, namely, region I of $0 < y < l$ and region II of $(L - l) < y < L$, and vanishing in region III of $l < y < (L - l)$. The system as a whole has a bulk energy gap around energy 0, for $g_0 \neq \pm M_0$. The edge states in the bulk energy gap can be solved analytically by replacing k_y with $-i\partial_y$ in the system Hamiltonian. For $\tau_z = 1$, an edge mode with energy $E_+(k_x) = -v_{\rm F}k_x$ is found on one side of the strip, whose wavefunction is given by

$$\varphi_+(k_x, y) = |1, -1\rangle\phi_+(k_x, y) \ . \qquad (3)$$

Here, ket $|\tau_z, \sigma_x\rangle$ with $\tau_z = \pm 1$ and $\sigma_x = \pm 1$ is used to represent the common eigenstate of $\hat{\tau}_z$ and $\hat{\sigma}_x$. The spatial wavefunction $\phi_+(k_x, y) = C[e^{-y/\xi_1(g)} - e^{-y/\xi_2(g)}]$ for $y < l$, and $\phi_+(k_x, y) = D_1 e^{-(y-l)/\xi_1(0)} - D_2 e^{-(y-l)/\xi_2(0)}$ for $y \geq l$, with C, D_1 and D_2 to be determined from the conditions of continuity and normalization of $\phi_+(k_x, y)$. The two characteristic length functions are defined as

$$\xi_{1,2}(\epsilon) = \frac{2B}{v_{\rm F} \pm \sqrt{v_{\rm F}^2 - 4B(M_0 - Bk_x^2 + \epsilon)}} \ . \qquad (4)$$

For $\tau_z = -1$, we find another edge mode with energy $E_-(k_x) = v_{\rm F}k_x$ and wavefunction

$$\varphi_-(k_x, y) = |-1, -1\rangle\phi_-(k_x, y) \ , \qquad (5)$$

where $\phi_-(k_x, y) = E[e^{-y/\xi_1(-g)} - e^{-y/\xi_2(-g)}]$ for $y < l$, and $\phi_-(k_x, y) = F_1 e^{-(y-l)/\xi_1(0)} - F_2 e^{-(y-l)/\xi_2(0)}$ for $y \geq l$. Owing to the two-fold rotation symmetry, the edge modes on the other side of the strip have dispersion relations $E_\pm(k_x) = \pm v_{\rm F}k_x$. Their wavefunctions can be obtained through replacements $y \to L - y$, $\sigma_x \to -\sigma_x$ and $k_x \to -k_x$ in Eqs. (3) and (5). The energy spectrum of edge states appears to have mirror symmetry between k_x and $-k_x$. However, this is an accidental event, and the system does not possess mirror symmetry if $g_0 \neq 0$.

In Eqs. (3) and (5), the $\hat{\boldsymbol{\tau}}$ and $\hat{\boldsymbol{\sigma}}$ parts of wavefunctions do not change with varying g_0. In Fig. 2(a), the

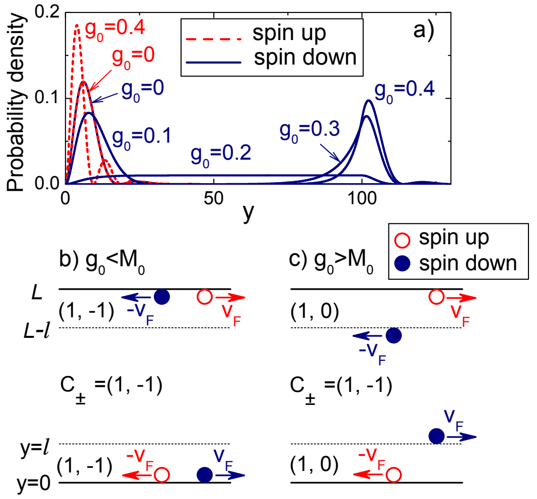

FIG. 2: (a) $|\phi_+(k_x, y)|^2$ and $|\phi_-(k_x, y)|^2$ at $k_x = 0$ as functions of y for different g_0, where $v_F = 1$, $B = 5$, $M_0 = 0.2$, and $l = 100$ are taken. Here, $|\phi_+(k_x, y)|^2$ is plotted only for two values of g_0, as its change with g_0 is relatively small. Spatial distributions of spin Chern numbers $C_\pm$ and edge states are shown for $g_0 < M_0$ (b) and $g_0 > M_0$ (c).

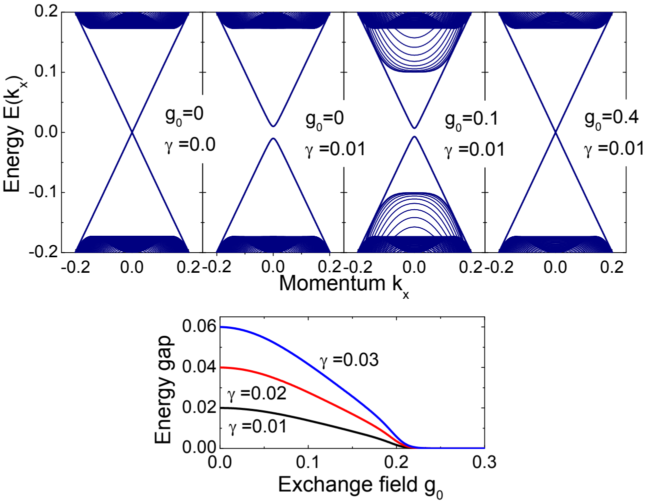

FIG. 3: Upper panel: calculated energy spectra for four sets of g_0 and γ. Lower panel: magnitude of the energy gap of edge states as a function of g_0 for three values of γ. The other parameters are taken to be $v_F = 1$, $B = 5$, $M_0 = 0.2$, $L = 1000$, and $l = 200$.

modulus squared of spatial wavefunctions $\phi_+(0, y)$ and $\phi_-(0, y)$ are plotted as functions of y for several values of g_0. The Fermi velocity v_F is taken to be the unit of energy. At $g_0 = 0$, we have $|\phi_+(0, y)|^2 = |\phi_-(0, y)|^2$, and both lines coincide with each other, which is required by the TR symmetry at $g_0 = 0$, as mentioned above. With increasing g_0, the peak of $|\phi_+(0, y)|^2$ becomes sharper and closer to $y = 0$. On the contrary, the shape of $|\phi_-(0, y)|^2$ widens with increasing g_0, and spreads across region I at $g_0 = M_0 = 0.2$. With further increasing g_0, $|\phi_-(0, y)|^2$ becomes localized near $y = l = 100$, i.e., the inner boundary of region I. This transition is directly caused by the sign change of $\xi_2(-g)$ in $\phi_-(0, y)$ at $g_0 = M_0$, from positive to negative. The other characteristic lengths in $\phi_+(0, y)$ and $\phi_-(0, y)$ remain positive during this process.

The evolution of the edge states with varying g_0 is further illustrated in Figs. 2(b) and 2(c), and can be understood in terms of calculated spin Chern numbers. For $g_0 < M_0$, the spin Chern numbers $C_\pm$ in the three regions take the same value $(1, -1)$. This indicates that the three regions are topologically equivalent, and can be regarded as a QSH system as a whole. As a result, the edge states for both up spin ($\tau_z = 1$) and down spin ($\tau_z = -1$) appear near the sample boundaries $y = 0$ and $y = L$, as shown in Fig. 2(b). For $g_0 > M_0$, the situation is quite different, because $C_\pm$ undergo a transition at $g_0 = M_0$ from $(1, -1)$ to $(1, 0)$ in regions I and II. For the spin-up electrons, the three regions have the same Chern number $C_+ = 1$, and as a whole are equivalent to a QH system. Therefore, the spin-up edge states remain localized near $y = 0$ and $y = L$. For the spin-down electrons, region III with $C_- = -1$ is a QH system, sandwiched between two insulators in regions I and II, where $C_- = 0$. The spin-down edge states thus shift to their interfaces, namely, $y = l$ and $y = L - l$, as shown in Fig. 2(c).

Comparing Fig. 2(c) for $g_0 > M_0$ with Fig. 2(b) for $g_0 < M_0$, one finds that both systems have very similar edge states: the lower edge contains a left mover with up spin and a right mover with down spin, and conversely for the upper edge, so as to exhibit the same QSH effect. An important difference is that for $g_0 > M_0$, the counterflows of electrons at the lower (upper) edge are spatially separated into two different "lanes" located at $y = 0$ ($y = L$) and $y = l$ ($y = L - l$), which provides an essential protection. [30] As a result, the QSH state for $g_0 > M_0$ should be more stable than that for $g_0 < M_0$. To show this point, we introduce a specific perturbation violating the TR symmetry. Since the two edge states given by Eqs. (3) and (5) have opposite τ_z, we include an in-plane Zeeman field throughout the sample with potential

$$V = \gamma \hat{\tau}_y \ , \tag{6}$$

which represents a "maximal" coupling between the two edge states near the degenerate point. A tight-binding model on a square lattice is constructed for the strip geometry, which recovers the form of Eq. (1) in the continuum limit. The energy spectrum is calculated numerically from the tight-binding model.

The calculated energy spectra for four sets of g_0 and γ are plotted in Fig. 3. Since the dispersion relation for edge states is given by $E_\pm(k_x) = \mp v_F k_x$ on one side of the strip and $E_\pm(k_x) = \pm v_F k_x$ on the other side, the energy spectra of edge states on the two sides collapse, and only two branches of edge states are seen in each

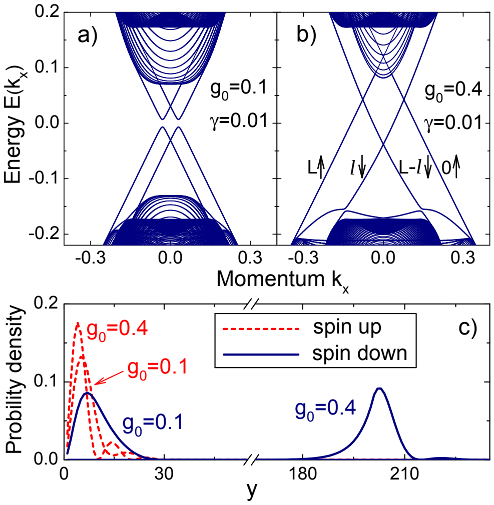

FIG. 4: Calculated energy spectra with $\gamma = 0.01$ and $g_1 = 0.3g_0$ for $g_0 = 0.1$ (a) and $g_0 = 0.4$ (b), and spatial probability distributions of the two edge states near the lower edge at energy $E = -0.01$ for $g_0 = 0.1$ and 0.4 (c). The other parameters are the same as in Fig. 3. Here, spin up and spin down refer to the edge states with positive and negative spin polarizations $\langle \hat{\tau}_z \rangle$, as $\hat{\tau}_z$ is not conserved.

figure. For $g_0 = \gamma = 0$, the edge states are gapless, as the system is TR invariant, and $\hat{\tau}_z$ is conserved as well. Upon turning on $\gamma = 0.01$, an energy gap appears in the edge state spectrum even at $g_0 = 0$, signaling the onset of backscattering. With increasing g_0 to 0.1, the energy gap decreases but remains finite. With further increasing g_0 to 0.4, greater than $M_0 = 0.2$, the energy gap vanishes, an indication of quenching of backscattering. The magnitude of the energy gap of the edge states is plotted as a function of g_0 in the lower panel of Fig. 3, for three different values of γ. While it increases almost proportionally to γ, the energy gap decreases with increasing g_0. When g_0 slightly exceeds the critical point $M_0 = 0.2$, the energy gap essentially vanishes for all the three values of γ. Furthermore, we find that for $g_0 < M_0$, the spin polarizations of the edge states $\langle \hat{\tau}_z \rangle$ deviate from ± 1 appreciably near the energy gap, as nonzero γ destroys the conservation of $\hat{\tau}_z$, but nearly full spin polarizations are restored for $g_0 > M_0$. These numerical results confirm our argument that the QSH effect in the $g_0 > M_0$ region is robust against general perturbations without symmetry constraints.

Finally, we investigate the effect of nonzero g_1 in the Hamiltonian on the QSH effect. Nonzero g_1 together with g_0 is present in FM regions I and II of Fig. 1. The calculated energy spectra are plotted in Fig. 4 for $g_0 = 0.1$ and 0.4, with $g_1 = 0.3g_0$ set in proportion to g_0. The energy spectra of edge states on the two sides of the strip are no longer degenerate in the presence of nonzero g_1, the positions and spin orientations of the split edge states being labeled in Fig. 4(b). Inclusion of nonzero g_1 also breaks the particle-hole symmetry. It is found that the edge states are gapped for $g_0 = 0.1$ ($< M_0$) and become gapless for $g_0 = 0.4$ ($> M_0$), respectively, shown in Figs. 4(a) and 4(b). The spatial probability distributions of the two edge states at $E = -0.01$ on one side of the strip are plotted in Fig. 4(c). While the spin-up polarized edge state stays near $y = 0$, the spin-down polarized edge state moves from near $y = 0$ to $y = l = 200$ with tuning g_0 from 0.1 to 0.4, exhibiting the same transition as in Fig. 2(a). This result indicates that the presence of nonzero g_1 does not change the physical picture qualitatively, and the robust QSH effect can be achieved when the exchange field is sufficiently strong.

This work is supported by the State Key Program for Basic Researches of China under Grants Nos. 2009CB929504 (LS), 2011CB922103, and 2010CB923400 (DYX), the National Natural Science Foundation of China under Grant Nos. 11225420, 11074110 (LS), 11023002 (BW), 11174125, 11074109, 91021003 (DYX), and a project funded by the PAPD of Jiangsu Higher Education Institutions. We also thank the US NSF Grants No. DMR-0906816 and No. DMR-1205734, and Princeton MRSEC Grant No. DMR-0819860 (DNS).

---

[*] Electronic address: shengli@nju.edu.cn
[†] Electronic address: dyxing@nju.edu.cn

[1] C. L. Kane and E. J. Mele, Phys. Rev. Lett. **95**, 226801 (2005).
[2] B. A. Bernevig, and S. C. Zhang, Phys. Rev. Lett. **96**, 106802 (2006).
[3] B. A. Bernevig, T. L. Hughes, and S. C. Zhang, Science **314**, 1757 (2006).
[4] M. König, *et al.*, Science **318**, 5851, 766 (2007).
[5] F. D. M. Haldane, Phys. Rev. Lett. **61**, 2015 (1988).
[6] L. Sheng, D. N. Sheng, C. S. Ting, and F. D. M. Haldane Phys. Rev. Lett. **95**, 136602 (2005).
[7] C. Wu, B. A. Bernevig, and S. C. Zhang Phys. Rev. Lett. **96**, 106401 (2006).
[8] C. L. Kane, and E. J. Mele, Phys. Rev. Lett. **95**, 146802 (2005).
[9] D. N. Sheng, Z. Y. Weng, L. Sheng, and F. D. M. Haldane, Phys. Rev. Lett. **97**, 036808 (2006).
[10] E. Prodan, Phys. Rev. B **80**, 125327 (2009); E. Prodan, New J. Phys. **12**, 065003 (2010).
[11] H. C. Li, L. Sheng, D. N. Sheng, and D. Y. Xing, Phys. Rev. B **82**, 165104 (2010).
[12] J. E. Moore, and L. Balents, Phys. Rev. B **75**, 121306 (R) (2007).
[13] L. Fu and C. L. Kane, Phys. Rev. B **76**, 045302 (2007); L. Fu, C. L. Kane, E. J. Mele, Phys. Rev. Lett. **98**, 106803 (2007).
[14] H. J. Zhang, C. X. Liu, X. L. Qi, X. Dai, Z, Fang, and S. C. Zhang, Nature Phys. **5**, 438(2009).
[15] M. Z. Hasan and C. L. Kane, Rev. Mod. Phys. **82**, 3045 (2010).
[16] X. L. Qi and S. C. Zhang, Physics Today. **63**, 33 (2010).
[17] L. Fu and C. L. Kane, Phys. Rev. Lett. **100**, 096407

(2008).

[18] X. L. Qi, T. Hughes, and S.-C. Zhang, Phys. Rev. B **78**, 195424 (2008).

[19] A. M. Essin, J. E. Moore, and D. Vanderbilt, Phys. Rev.

[20] D. Hsieh, *et al.*, Nature **452**, 970 (2008); D. Hsieh, *et al.*, Science **323**, 919 (2009).

[21] Y. Xia, et al., Nature Physics 5, 398 (2009).

[22] H. Zhang, C. Liu, X. Qi, X. Dai, Z. Fang, and S. Zhang, Nature Physics **5**, 438 (2009).

[23] Y. L. Chen, *et al.*, Science **325**, 178 (2009).

[24] P. Roushan, *et al.*, Nature **460**, 1106 (2009).

[25] T. Zhang, *et al.*, Phys. Rev. Lett. **103**, 266803 (2009). Lett. 102, 146805 (2009).

[26] Y. Yang, Z. Xu, L. Sheng, B. G. Wang, D. Y. Xing, and D. N. Sheng Phys. Rev. Lett. **107**, 066602 (2011); H. C. Li, L. Sheng, and D.Y. Xing, Phys. Rev. Lett. **108**, 196806 (2012).

[27] C.-X. Liu, X.-L. Qi, X. Dai, Z. Fang, and S. C. Zhang, Phys. Rev. Lett. 101, 146802 (2008).

[28] C. Brüne, *et al.*, Phys. Rev. Lett. **106**, 126803 (2011).

[29] W.-Y. Shan, H.-Z. Lu, S.-Q. Shen, New J. Phys. **12**, 043048 (2010); H.-Z. Lu, W.-Y. Shan, W. Yao, Q. Niu, and S.-Q. Shen, Phys. Rev. B **81**, 115407 (2010).

[30] A random potential without symmetry constraints takes the general form $U(\mathbf{r}, \hat{\boldsymbol{\sigma}}, \hat{\boldsymbol{\tau}})$. Its matrix element between two counterpropagating edge states is given by $\langle \varphi_+(k_x, y)|U|\varphi_-(-k_x, y)\rangle = \int dy \phi_+^*(k_x, y)\phi_-(-k_x, y)\mathcal{U}(2k_x, y)dy$ with $\mathcal{U}(2k_x, y) = \int \frac{dx}{2\pi} e^{-2ik_x x}\langle 1, 1|U(\mathbf{r}, \hat{\boldsymbol{\sigma}}, \hat{\boldsymbol{\tau}})| -1, -1\rangle$. Since $\phi_+(k_x, y)$ and $\phi_-(-k_x, y)$ are exponentially localized near $y = 0$ and $y = l$, respectively, the matrix element vanishes exponentially for sufficiently large l, and so backscattering is prohibited.